SMAR 2019 – Fifth Conference on Smart Monitoring,
Assessment and Rehabilitation of Civil Structures

SMAR 2019

Experimental investigation on physico-mechanical properties of natural building stones exposed to high temperature

Martin VIGROUX [1], Javad ESLAMI [1], Anne-Lise BEAUCOUR [1], Ann BOURGÈS [2], Albert NOUMOWÉ [1],

[1] Laboratoire de Mécanique et Matériaux du Génie Civil - Université de Cergy-Pontoise, Cergy-Pontoise, France

[2] Laboratoire de Recherche des Monuments Historiques - Ministère de la Culture et de la Communication, Champs-sur-Marne, France

Contact e-mail: martinvigroux@gmail.com

ABSTRACT: Fire has always been a major threat to building and consequences can then be dramatic. Since natural stones were frequently used as building material in historical monuments, a detailed understanding of thermal damage and failure mechanical behavior of these porous materials at elevated temperature is a key concern. When exposed to fire, natural stones can suffer from irreversible changes in microstructure and mechanical properties. These disorders may compromise the structural integrity and increase the risk of instability of the entire building. Thereby, the aim of this study is to understand the effect of fire and identify important changes that occur when selected building stones are experimentally heated up to 200, 400, 600 and 800 °C. Therefore, stones with different mineralogy and various physical characteristics are tested after each exposure. Then, damage evolution is determined through measurement of physico-mechanical properties such as compressive strength, Young modulus, tensile strength, porosity, P-wave velocity.

1 INTRODUCTION

Natural stones have been used for a long time as building materials, and are still used as restoration materials De Kock et al. (2014). Historical monuments are not spared by fires and the consequences can be disastrous. Thus, fire always appears as one of the main causes of weathering because it can generate irreversible damage with long-lasting effects, in a very short period of time. Then, studying the impact of fire on stone is therefore of great importance : fire can cause a significant decline in the strength of stone, lead to loss of surface material and may compromise the structural integrity of a building Gómez-Heras et al. (2009). Several authors studied the effect of high temperature on mechanical properties Chaki et al. (2008), transport properties Rodríguez-Gordillo et al. (2006) but also colour change on different type of stones Ozguven et al. (2013). In this present work, seven stones from French active quarries were experimentally heated up to four different heating-cooling cycles. Then, residual physico-mechanical tests were performed to determine the intrinsic parameters governing the sensitivity to high temperature. Furthermore, tests under high temperature such as thermogravimetric analysis but also thermal linear expansion tests were conducted in order to establish the physico-chemical and thermo-mechanical behaviour of these materials when subjected to 1000 °C. Due to this coupled analysis, this study brings new elements on the explanation of the damage mechanisms and highlights the most influent parameters on high temperature behavior.

2 MATERIALS AND METHODS

2.1 Stones description

The seven stones used in this study are all from active quarries, located in different regions of France. Six of them are classified as limestones : Massangis (MA), Lens (LS), Euville (EUV), Migné (MI), Saint Maximin (MX), Savonnières (SA) while the seventh one is a sandstone from North-East of France : Grès des Vosges (GR). These stones have been chosen because they have been widely used in the construction of historical monuments and are still used for restoration purposes. Moreover, they present a vast variety of physical, mechanical and microstructure properties but also involve different mineralogy. Indeed, X-ray diffraction analysis performed on these seven stones at initial state suggest that LS, EUV, MI and SA are purely calcite while MX is made of 90% of calcite and 10% of quartz. MA is composed of a dominant calcite-dolomite phase and a small amount of quartz (3%). The sandstone GR has a high quartz content 80%, with K-feldspar (microcline) and iron oxide 15% and a very low clay-content matrix : illite and kaolinite (5%). The combined use of Figure 1 (b) showing the relative proportion of the different constitutive phases for the six limestones, based on a 300 point-counting analysis on thin sections, with Figure 1 (a) presenting the grain size distribution, clearly showcases the large variety of stones used in this study, in terms of texture and microstructure.

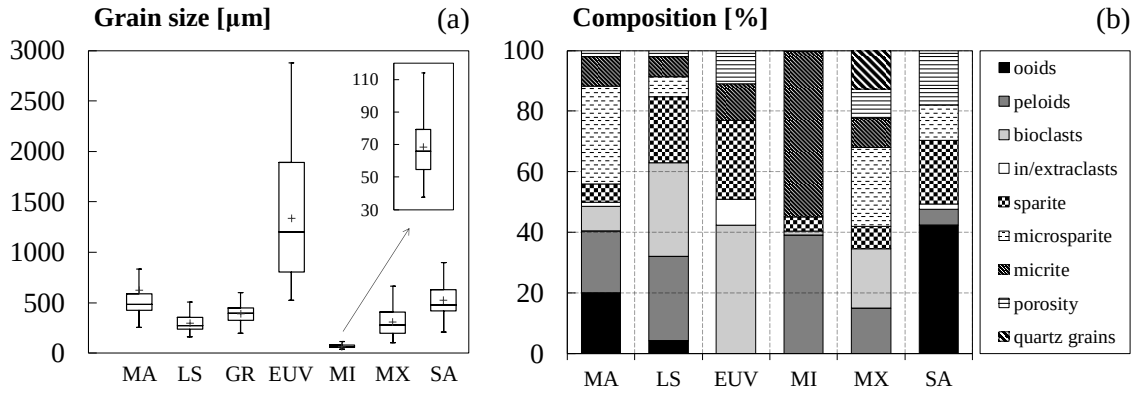

Figure 1. Grain size distribution for the seven stones (a) and relative proportion of the different constitutive phases for the six limestones (b) at initial state.

EUV limestone is a bioclastic grainstone, composed of multi-millimetric elements (500 to 2800 µm) with a calcite crystals matrix. On the contrary, MI stone is a peloidal packstone formed almost exclusively of peloids (50 to 100 µm) in a very fine micrite matrix. MA, LS, MX and SA limestones display a similar grain size range (250 to 800 µm), and these last two stones with EUV, have a large porosity. GR sandstone is a felspathic litharenite mainly composed of quartz grains (400 µm), but also with an important part of various lithoclasts.

These seven stones differ from each other by their mineralogical composition, microstructure and thus also with physical and mechanical properties. Table 1 lists the main characteristics of stones at initial state. Then, SA, MX and MI limestones have similar properties : high porosity greater than 25%, accompanied by low mechanical properties, with R_C ranging from 10 to 20 MPa. GR, EUV and LS are less porous, but present disparities in mechanical properties : R_C ranging from 20 to 47 MPa. On the contrary, MA stone, with the lowest porosity, has the highest density and mechanical properties.

Table 1. Main physical and mechanical properties of stones at initial state : total water porosity N_T, density ρ, uniaxial compressive strength R_C, undirect tensile strength R_T, dynamic Young's modulus E_{dyn} and P-wave velocity V_P

Name	N_T [%]	ρ [kg.m^{-3}]	R_C [MPa]	R_T [MPa]	E_{dyn} [GPa]	V_P [m.s^{-1}]
Massangis	11,2 ± 0,5	2391 ± 11	74 ± 1,5	8,7 ± 0,7	45 ± 1,4	4941 ± 192
Lens	15,4 ± 0,8	2252 ± 23	27 ± 1,5	5,3 ± 0,4	32 ± 1,9	4380 ± 172
Grès	15,7 ± 2,2	2220 ± 58	47 ± 1,6	5,2 ± 0,6	17 ± 2,5	3067 ± 195
Euville	17,2 ± 0,4	2209 ± 15	20 ± 0,5	3,5 ± 0,2	23 ± 1,1	3665 ± 359
Migné	26,8 ± 0,8	1949 ± 22	20 ± 3,0	2,7 ± 0,4	15 ± 1,1	3138 ± 95
Saint Maximin	29,7 ± 1,2	1791 ± 23	15 ± 1,2	2,0 ± 0,1	12 ± 0,8	2971 ± 124
Savonnières	30,7 ± 1,3	1786 ± 25	9 ± 0,6	1,6 ± 0,1	12 ± 0,9	2984 ± 119

2.2 Experimental procedures

In order to investigate the mass evolution during heating, thermogravimetric analysis were conducted under a nitrogen atmosphere using a STA 449 F1 Jupiter device developed by Netzsch. Powder samples for each stone were obtained from dry specimens, placed in an 80 °C oven for 72 hours, and then heated from room temperature to 1000 °C at a rate of 4 °C/min. Moreover, thermal linear deformation was recorded using a Pushrod dilatometer DIL 402 C by Netzsch. These tests were performed on three dry cylindrical samples of Φ10 × 50 mm in length for each stone. The heating program is the same as the one used for TGA analysis : 4 °C/min up to 1000 °C. An electric furnace with a 1,35 m3 capacity was used. The two side walls are equipped with heating resistors and a ventilator is located at the back of the furnace to maintain a homogeneous temperature distribution. Type-K thermocouples were positioned at different positions to verify these conditions. Four different high temperature treatments were applied on samples through heating-cooling cycles : from room temperature to 200, 400, 600 and 800 °C. Each treatment includes a 4 °C/min heating phase up to target temperature, then a one-hour isotherm stage and finally a semi-forced cooling phase. The low heating rate ensures the homogeneity of temperature and limits the thermal gradient in the specimen according to RILEM TC 200-HTC. With the aim of investigating the effect of heat treatment on the studied stones, several tests were performed after these 4 heating programs to analyze the evolution of physico-mechanical properties. Then, uniaxial compression test was carried out on three cylindrical Φ40 × 80 mm specimens according to standards NF EN 1926 in order to determinate the compressive strength R_C. A constant strain rate 100 µm/min was applied with an electromechanical static load cell Intron Press 30 kN. Brazilian indirect tensile test was achieved with the same device on four cylindrical Φ40 × 40 mm specimens according to standards NF P 94-422 to obtain the tensile strength R_T. The strain rate was maintained constant 1 kN/min until the failure. These two mechanical tests were carried out for each stone at initial state and after the four different high temperature treatments. The porous network was investigated by using total water porosity under vacuum technique. Total porosity N_T test was carried out according to standards NF EN 1936 on 40 intact samples for each stone, and thereafter on 6 samples after heat treatments. This test also enables the determination of dry density ρ. Measurements of P-wave velocity V_P were performed using a Pundit7, a wave propagation test device from Pundit Lab, according to standards NF EN 14 579. The average values for each stone are based on 60

samples (Φ40 × 80 mm) for initial state and based on 10 to 12 samples after high temperature treatments. This test gives information on microcracking state inside the sample and the dynamic Young's modulus Edyn is thus determined using dry density ρ and Poisson's ratio υ at corresponding temperature.

3 RESULTS AND DISCUSSION

3.1 Thermogravimetric analysis

Figure 2 shows the evolution of mass loss for the seven studied stones as a function a temperature up to 1000 °C. The general trend for the six limestones is a stable thermal phase until 750 °C where the decarbonation of calcite $CaCO_3 \rightarrow CaO + CO_2$, occurs and leads to an approximately 45% mass loss when the chemical reaction is complete (950 °C). It should be noted that EUV limestone presents an earlier mass loss (2% starting at 370 °C) that is explained by Homand-Etienne (1986) either by its organic matter content or by the presence of hydrates. Furthermore, the presence of dolomite in MA limestone, is observable through its decomposition reaction $CaMg(CO_3)_2 \rightarrow CaCO_3 + MgO + CO_2$ which starts earlier at 650 °C. Concerning GR sandstone, it doesn't appear any significant mass loss (1% at 1000 °C) since the α-β phase transition of quartz at 573 °C is not associated with a loss of matter.

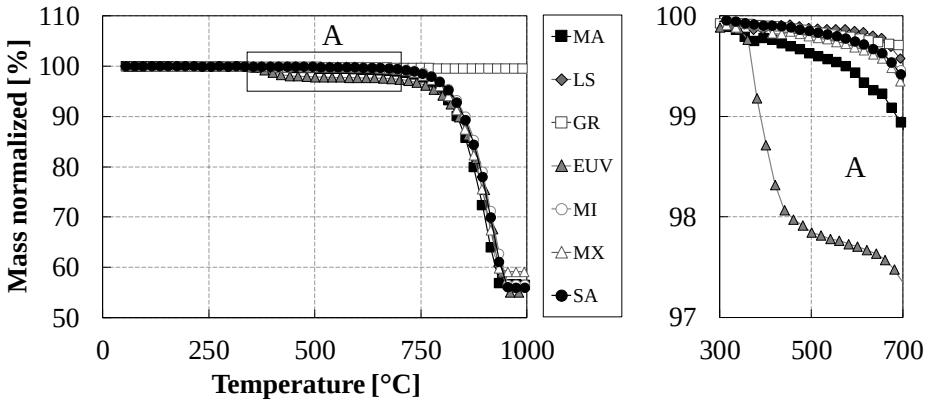

Figure 2. Evolution of mass as a function of temperature up to 1000 °C.

3.2 Thermal linear deformation

The thermal linear deformation for the 7 stones is presented in Figure 3 (a), and the coefficient of thermal expansion α, defined as the derivative of thermal strain with respect to temperature, is then displayed in Figure 3 (b). Figure 4 shows the detailed and individual curves of α for the 7 stones for a better visual perception. At first sight, and up to 500 °C, the seven stones expand parabolically but at different amplitude, especially for EUV. Thus, the thermal expansion coefficient α can be considered as increasing linearly with respect to temperature up to 550 °C, except for EUV stone which shows a maximum amplitude peak at 370 °C related to its mass loss (Figure 2). Its high coefficient α value 2,6 $\times 10^{-5}$ °C^{-1}, while 0,8-1,4 $\times 10^{-5}$ °C^{-1} for the other stones, seems to be attributed to its specific texture and large grain size (Figure 1). The presence of quartz leads to an important peak of α at 573 °C, temperature of α-β phase transition, for GR sandstone but also for MX limestone which contains 10% of quartz. After this temperature, GR doesn't show any strain evolution and stays stable (1,6%) up to 1000 °C. At 770 °C, calcite decarbonation reaction starts : deformation remains positive although α values decrease and results in the reversal of deformation kinetics. Thus, limestones finish their expansion phase

reaching a maximum peak around 850-900 °C, and then a contraction phase, associated with negative values of α, takes over up to 1000 °C.

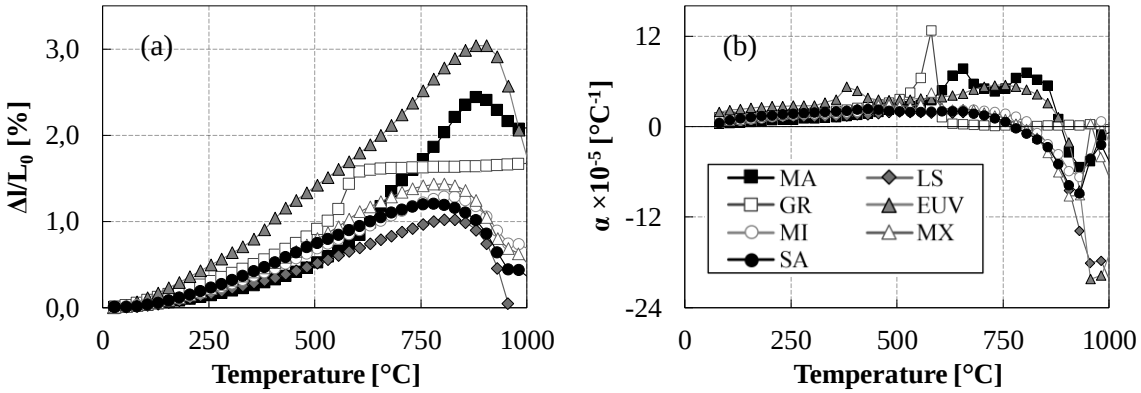

Figure 3. Thermal linear deformation (a) and thermal expansion coefficient (b) as a function of temperature up to 1000 °C.

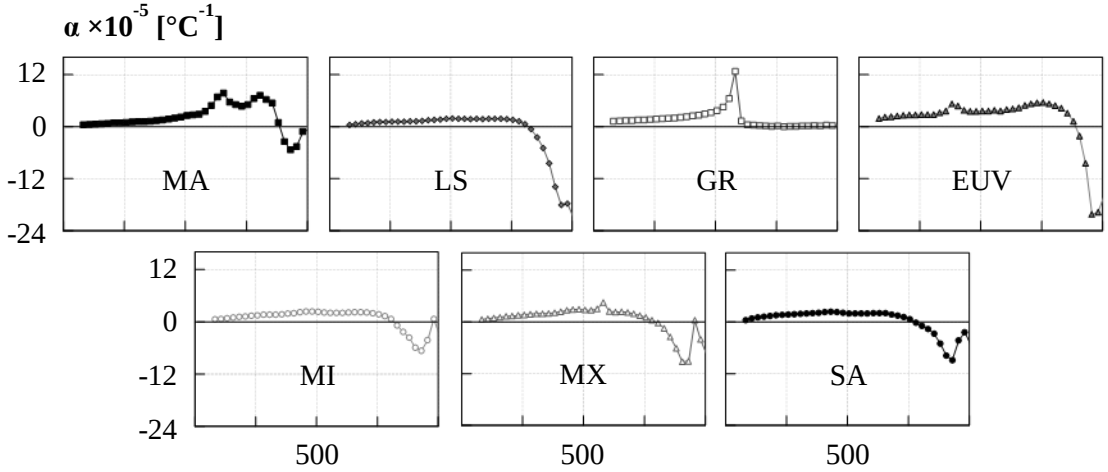

Figure 4. Detailed curves for each stone of thermal expansion coefficient up to 1000 °C.

3.3 Evolution of residual physico-mechanical properties after heating-cooling cycle

Figure 5 presents the relative evolution of residual properties up to 800 °C : uniaxial compressive strength R_C, undirect tensile strength R_T, dynamic Young's modulus E_{dyn} and total porosity increase ΔN_T after the four different heating-cooling cycles. Regarding the thermal evolution of mechanical parameters R_C and R_T, it can be stated that a 200 °C heating treatment does not affect significantly these stones. Indeed, only a maximum loss of 8% is observable, except for EUV limestone that already presents a 20% loss of tensile strength R_T at 200°C. After this first target temperature, the relative evolution of R_C and R_T shows a slight difference : loss in compressive strength R_C does not exceed 10% at 400 °C (except EUV) while tensile strength R_T starts to decrease in a more significant way, between 10 and 30%, for respectively SA and LS limestones, and even more for EUV with an important loss of 80%. At 600 and 800 °C, the general evolution trend appears to be quite similar for R_C and R_T. GR sandstone and more particularly MI limestone seem to be the least affected by these thermal loadings : respective loss of 20-30% for R_C, and 40-50% for R_T at 800 °C. On the contrary, EUV stone is by far the

least resistant to heat treatments : it is clearly highlighted by a considerable loss of more than 80% in R_T and 60% in R_C.

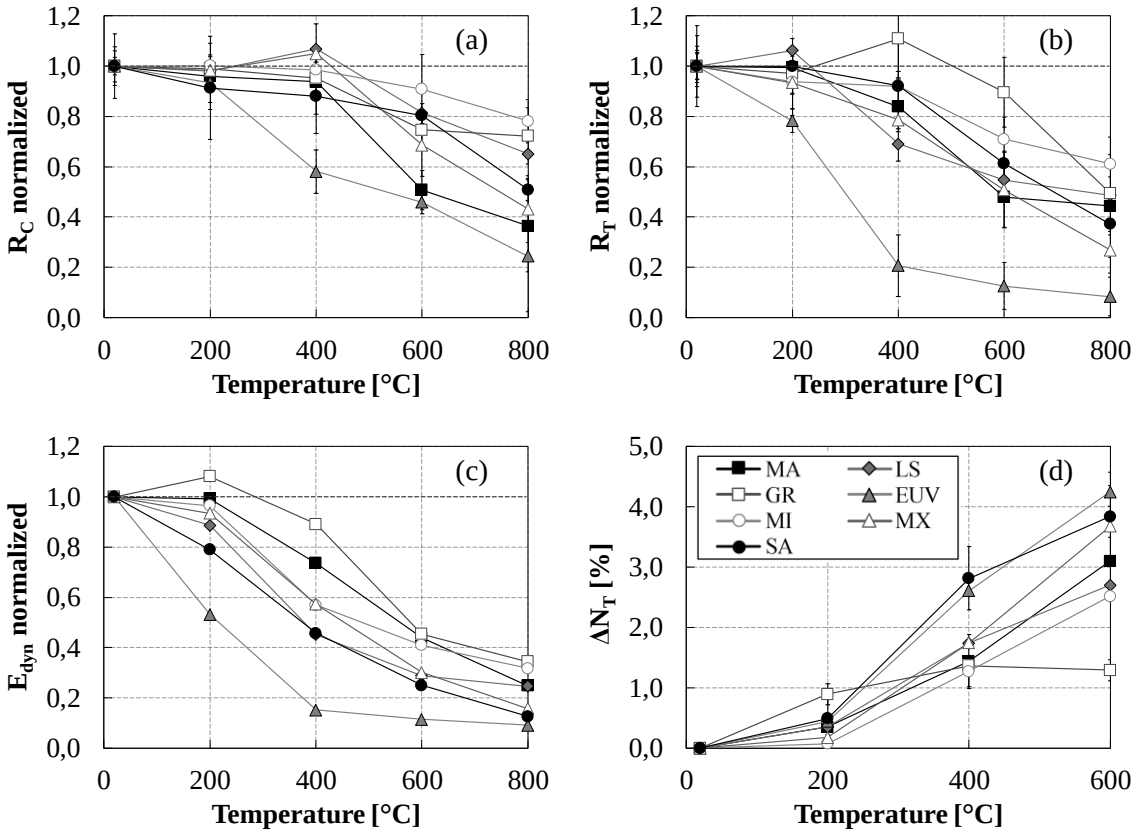

Figure 5. Thermal relative evolution of residual properties up to 800 °C : uniaxial compressive strength R_C (a), tensile strength R_T (b), dynamic Young's modulus E_{dyn} (c) and total porosity increase ΔN_T (d).

The relative evolution of dynamic Young's modulus E_{dyn} illustrate a similar trend as that observed for the failure strengths. EUV appears as very sensitive to the elevated temperatures and exhibits thermal damage that develops at lower temperature (200 °C) than the other stones. Indeed, after a first and significant loss at 200 °C, E_{dyn} decreases linearly from 400 °C up to 800 °C. As for R_C and R_T, the evolution of dynamic modulus of GR and MI confirms that these stones are the most robust ones facing high temperature exposure. Changes in porosity either are related to the occurence of micro-cracks as a result of dimension and shape changes induced by differential expansion or, are driven by structural collapse of minerals. GR stone exhibits the lowest increase in porosity below 1,5%. In contrast to the limestones, its evolution is not linear and porosity no longer increases beyond 400 °C. Increase in porosity of MI, LS and MA stones ranges from 2,5 to 3,0% at 600 °C. The highest porosity increases at 600 °C are observed for EUV with 4,2% and then for SA and MX with 3,8%. The early thermal damage developed in EUV stone may result in two main factors : its anisotropic and granular structure, with a very heterogeneous and large grain size distribution that causes a much higher thermal expansion than the other stones. Moreover, the second element is the early loss of mass that occurs at 370 °C. These two combined features tend to make EUV as very sensitive to high temperature since losing a significant part of physico-mechanical performances. MA and MX limestones both contain a second type of minerals in a relative proportion, dolomite and quartz, respectively. This second mineralogy element content seems to have an unfavorable influence on the

evolution of mechanical properties since MX stone, for example, presents a significant and sharp loss of property especially at 600 °C, just after 573 °C, α-β phase transition of quartz. The quartz phase transition is accompanied with the increase in volume in quartz grains resulting in stress increase and therefore micro-cracks occurence. Cracking is worsened by a large difference in the thermal dilatation between quartz and calcite.

3.4 Assessment of structural stability and kinetics of disintegration

It is essential to investigate the post-cooling behaviour of natural building stones exposed to high temperature and how it evolves over time after an 800 °C heating in order to establish safety precautions, and then determinate the nature of restoration work Ozguven et al. (2013).

Therefore, a special attention was paid to follow the damage state of the seven samples exposed to 800 °C. Figure 6 represents the six limestone samples, 30 minutes after being removed from the furnace. GR sandstone is not displayed since it shows a great structural stability and no macroscopic crack can be observed. In addition, crack density η was calculated using image analysis on 3 sample surfaces and is presented in Table 2. Many macroscopic cracks are visible and EUV is statistically the most surface-damaged stone since it presents a high crack density. SA and MX also show a well-developed cracks network. MI and MA exhibit a similar value while LS is only slightly affected by crack development. These parameter values corroborate the observations about the evolution of the residual physico-mechanical properties (Figure 5).

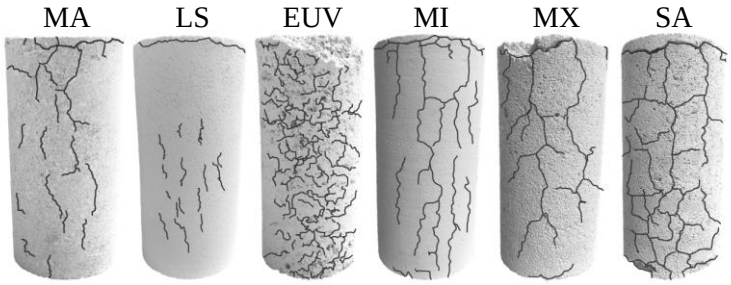

Figure 6. Limestone specimens after 800 °C heating treatment (30 minutes after being removed from the furnace) – black lines represent the macroscopic cracks that can be easily identified.

Table 2. Crack density per unit area η of specimen surfaces after 800 °C heating treatment

Name	MA	LS	EUV	MI	MX	SA
η [cm/cm²]	1,04 ± 0,08	0,65 ± 0,04	2,51 ± 0,26	1,06 ± 0,12	1,24 ± 0,15	1,91 ± 0,19

Figure 7 displays the evolution of the same six limestone specimens shown on Figure 6, but after a 24-hour exposure in a HR and temperature-monitored room (50%, 20 °C). Samples were hand-manipulated in order to evaluate the degree of brittleness and consequently determine if those stones could still ensure their role of load-bearing material. MA, LS and MI limestones are the most resistant even though these three stones present a crumbly texture on surface, and is even divided in two pieces for MI. Indeed, when lime obtained by calcite decarbonatation reacts with some atmospheric water vapour, there is formation of portlandite, a calcium hydroxide, according to $CaO + H_2O \rightarrow Ca(OH)_2$, which leads to a considerable volume increase causing in some cases the total disintegration of specimen. EUV, SA and MX limestones are totally destroyed just 24 hours after the end of the 800 °C heating. These experimental observations highlight the problem that some natural limestone used as building material could be facing

after the intervention of firefighters to extinguish a fire. This gives important indications regarding safety procedures considering a limited time available to secure the structure.

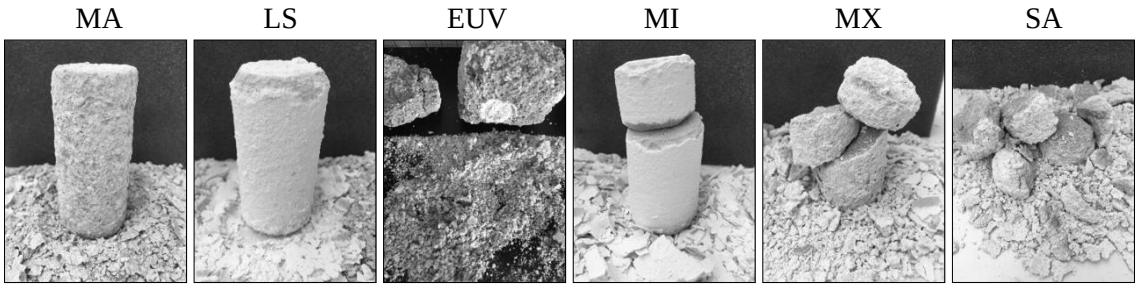

Figure 7. Assessment of structural stability for 800 °C heated samples after 24-hour exposure in a HR and temperature-monitored room – specimens were hand-manipulated for evaluation of disintegration.

4 CONCLUSION

The results indicate that natural stones can be highly affected by high temperature exposure but may exhibit different behaviors. Several intrinsic properties such as mineralogical composition, petrophysical and mechanical properties can be considered as the main parameters influencing on fire resistance. Overall, when heated until 400 °C, there is not a significant change in mechanical properties, except for one stone (EUV) due to its specific texture. However, exposure to higher temperatures leads to an important decrease in failure strengths. It is also noticed a sharp decrease in Young‘s modulus values and the porous network undergoes an extensive alteration through an increase in porosity. Despite a low heating rate and so without any significant thermal gradients, this reduction is related to intense thermal microcracking development inside the sample, caused by differential thermal deformation. Finally, thermogravimetric analysis show that mineralogical transformation such as calcite decarbonatation starts around 750 °C, and leads to a significant loss of mass, resulting in a sample contraction and a decrease of mechanical properties. In addition, exposure to atmospheric air after an 800 °C heating situation produces a chemical reaction causing disintegration of material : the structural stability is then highly unsettled.

5 ACKNOWLEDGEMENTS

The authors thank the “Fondation des Sciences du Patrimoine (EUR-17-EURE-0021)”.

6 REFERENCES

Chaki, S., Mokhfi T., and Agbodjan W. P., 2008, Influence of thermal damage on physical properties of a granite rock. *Construction and Building Materials*, 22: 1456–61.

Gómez-Heras, M., McCabe S., Smith B. J., and Fort R., 2009, Impacts of fire on stone-built heritage : an overview. *Journal of Architectural Conservation*, 15(2): 47–58.

Homand-Etienne, F., 1986, Comportement mécanique des roches en fonction de la température. *Phd, Université de Nancy, France.*

De Kock, T., Dewanckele, J., Boone, M., De Schutter, G., Jacobs, P., and Cnudde, V., 2014, Replacement stones for Lede stone in Belgian historical monuments. *The Geological Society of London*, 391: 31–46.

Ozguven, A., and Ozcelik Y., 2013, Investigation of some property changes of natural building stones exposed to fire and high heat. *Construction and Building Materials*, 38: 813–21.

Rodríguez-Gordillo, J., and Sáez-Pérez M. P., 2006, Effects of thermal changes on Macael marble : experimental study. *Construction and Building Materials*, 20: 355–65.